The Role of Angiotensin II/AT1 Receptor Signaling in Regulating Retinal Microglial Activation

Joanna A. Phipps, Kirstan A. Vessey, Alice Brandli, Nupur Nag, Mai X. Tran, Andrew I. Jobling, and Erica L. Fletcher

Department of Anatomy and Neuroscience, The University of Melbourne, Parkville, Australia

PURPOSE. This study explored whether the proangiogenic factor Angiotensin II (AngII) had a direct effect on the activation state of microglia via the Angiotensin type 1 receptor (AT1-R).

METHODS. Microglial dynamic activity was investigated in live retinal flatmounts from adult $Cx3Cr1^{+/GFP}$ mice under control, AngII (5 μM) or AngII (5 μM) + candesartan (0.227 μM) conditions. The effects of intravitreal administration of AngII (10 mM) were also investigated at 24 hours, with retinae processed for immunocytochemistry, flow cytometry, or inflammatory quantitative PCR arrays.

RESULTS. We found FACS isolated retinal microglia expressed AT1-R. In retinal flatmounts, microglia showed characteristic movement of processes under control conditions. Perfusion of AngII induced an immediate change in process length (-42%, $P < 0.05$) and activation state of microglia that was ameliorated by AT1-R blockade, suggesting a direct effect of AngII on microglia via the AT1-R. Intravitreal injection of AngII induced microglial activation after 24 hours, which was characterized by increased soma size (23%, $P < 0.001$) and decreased process length (20%, $P < 0.05$). Further analysis indicated a significant decrease in the number of microglial contacts with retinal neurons (saline 15.6 ± 2.31 versus AngII 7.8 ± 1.06, $P < 0.05$). Retinal cytokine and chemokine expression was modulated, indicative of an inflammatory retinal phenotype.

CONCLUSIONS. We show that retinal microglia express AT1-R and their activation state is significantly altered by the angiogenic factor, AngII. Specifically, AngII may directly activate AT1-Rs on microglia and contribute to retinal inflammation. This may have implications for diseases like diabetic retinopathy where increases in AngII and inflammation have been shown to play an important role.

Keywords: microglia, angiotensin II, retina, angiotensin receptor 1, inflammation

Microglia are the principal resident immune cells of the central nervous system (CNS), including in the retina.[1] Recent work has shown that microglia constantly survey the surrounding environment, extending and retracting their processes and making contacts with neurons, glial cells, and blood vessels.[2,3] In the presence of tissue insult or disease, microglia undergo an activation process, whereby they retract their processes and produce proinflammatory/chemotactic factors.[4] While the microglial-mediated immune response is critical to maintaining or re-establishing normal tissue function, an inappropriate or prolonged response can lead to pathology. For example, microglial-mediated inflammation has been implicated in a number of pathologies including Alzheimer's disease and multiple sclerosis,[5–7] while their response in the retina has been associated with the development of retinal degenerations such as age-related macular degeneration and diabetic retinopathy.[8,9] In particular, microglial mediated inflammation has been shown to lead to an upregulation in VEGF and Angiotensin II (AngII),[10,11] both of which have been shown to be integral in the development of vascular leakage and angiogenesis in diabetic and hypertensive retinopathy.

The vasoactive peptide hormone AngII is the main effector peptide of the renin–angiotensin system (RAS) and is responsible systemically for the control of blood pressure, salt appetite, and aldosterone formation.[12] It also plays an important role in angiogenesis in the retina and elsewhere in the body.[13,14] In these situations, AngII acts as a proangiogenic factor, causing blood vessel constriction,[15] vessel leakage,[16] migration of pericytes,[17,18] and upregulation of VEGF-induced endothelial cell proliferation.[19] In the retina, AngII is derived from a local RAS, most likely within the retinal glia as AngII cannot cross the blood–retinal barrier from the systemic circulation.[20] The effects of AngII are mostly mediated via the actions of the angiotensin receptor 1 (AT1-R), which to date has been primarily localized to glia and blood vessels in the retina.[21] While normally involved in retinal homeostasis, AngII levels have been shown to increase in the eye in diseases such as diabetic and hypertensive retinopathy.[22]

Very little is known about how AngII regulates glial–blood vessel function in the retina, and particularly whether it modulates retinal microglial signaling. Within the brain, AngII has been shown to play an active role in neuroinflammation associated with hypertension by causing activation of microglia,[23–25] and AT1-Rs have been localized to both macrophages and microglia.[26,27] This AngII-dependent activation of microglia results in the increased production of cytokine/proinflammatory factors within the brain,[23,25] and blockade of the AT1-R has

been shown to have broad anti-inflammatory effects, reducing tissue pathology and microglial activation and decreasing the production and release of a number of common proinflammatory cytokines.[28] These studies emphasize the important, yet relatively unexplored, nonvascular effects that AngII can exert within the CNS. While there is evidence of AngII-mediated activation of microglia and its role in modulating disease within areas of the brain, this possibility has not been investigated in the retina.

Given that AT1-Rs have been found on microglia in the brain, it is possible that retinal microglia are also under AngII/AT1-R control. In this paper, we investigate the localization of AT1-Rs to microglia in the retina, and explore the effects of AngII and AT1-R signaling on microglial activation state, phenotype, and downstream neuronal and inflammatory effects. Understanding the role of AT1-R/AngII signaling in relation to microglial activation has important implications for microglial–neuronal and microglial–vessel interactions in both normal physiological tissue and during disease.

METHODS

Animals

C57bl6J mice (wild-type mice) were obtained from the Animal Resource Center (West Australia). $Cx3cr1^{+/eGFP}$ mice on a C57bl6J background, which express enhanced green fluorescent protein (eGFP) under control of the endogenous $Cx3cr1$ locus,[29] were originally obtained from Paul McMenamin (Monash University, Australia). All mice were bred and housed at the University of Melbourne animal facility on a 12-hour light/dark cycle, with cage illumination <10 lux during the light period. Food and water were available ad libitum. All experiments adhered to the ethics committee standards of the University of Melbourne (Ethics no. 1313032) and the ARVO Statement for the Use of Animals in Ophthalmic and Vision Research.

Isolation of Retinal Microglia and Analysis of mRNA Expression

Adult C57bl6J animals were anaesthetized (ketamine 67 mg/kg and xylazine 13 mg/kg), overdosed with pentobarbitone sodium (120 mg/kg), and the eyes removed. The anterior segment was removed and the retina isolated and enzymatically digested (Papain Dissociation System; Worthington Biochemical Corporation, NJ, USA) to produce a single cell suspension. Microglia were incubated with Cd11b-FITC conjugated antibody (1:10; catalog #130-081-201, Miltenyi Biotec, NSW, Australia) and collected using fluorescence activated cell sorting (FACS; FACS Aria III, Becton Dickinson, Franklin Lakes, NJ, USA). Cells were collected directly into 600 μL lysis buffer (RLTplus; Qiagen, Valencia, CA, USA) containing 113 mM dithiothreitol, snap frozen in liquid nitrogen, and stored at −80°C. Total RNA was isolated from the microglial samples using commercial spin columns (RNeasy Micro Plus; Qiagen), reverse transcribed (Sensiscript; Qiagen), and amplified (55°C, 40 cycles, MyTaq; Bioline, NSW, Australia) using specific primers to $Agtr1a$ and b ($Agtr1a$, 5′-cataggactgggcc taacca-3′ and 5′-tgaatcagcacatccaggaa-3′; $Agtr1b$, 5′-atgaatctca gaactcaacac-3′ and 5′-aaaactgaatatttggtggga-3′). In order to assess the purity of the microglial isolation, amplifications were performed using primers to the microglial-specific gene $Cx3cr1$ (5′-ggccttgagcgacctgctctttg-3′ and 5′-gatgctgatgacggt gatgaagaa-3′) and photoreceptor gene Rho (5′-agcagcaggagt cagccacc-3′ and 5′-ccgaagttggagccctggtg-3′).

Confocal Time-Lapse Imaging of Retinal Explants

Five- to eight-week-old $Cx3cr1^{+/eGFP}$ mice were anaesthetized as above and retinae were dissected from the posterior eyecup. Retinae were placed photoreceptor side down on a ring of filter paper, which allowed central and midperipheral retina to be exposed. The mounted retinae were immediately placed ganglion cell layer (GCL) down onto a glass-coverslip bottomed petri-dish and perfused at 1 mL/min with carbogenated Ames medium (Sigma-Aldrich Corp., NSW, Australia) at 37°C. Retinal explants were imaged using an inverted confocal microscope (Leica SP5, Exton, PA, USA) with a ×40 oil objective and a zoom of 2. Ten-second z-stack images were collected at 512 × 512-pixel resolution.

Microglia were imaged for 30 minutes under three conditions: (1) Constant perfusion by carbogenated Ames at 1 mL/min for 30 minutes (six cells from five animals). (2) Ten minutes of Ames perfusion to obtain a baseline, followed by 10 minutes of 5 μM AngII at 1 mL/min, followed by a 10-minute Ames washout (10 cells, 5 animals). (3) Preincubation of 0.1 μg/mL candesartan, an AT1-R antagonist (0.227 μM; Sigma-Aldrich Corp.) in carbogenated Ames for 10 minutes to obtain a baseline, 10 minutes 5 μM AngII with 0.227 μM candesartan perfusion at 1 mL/min, followed by a 10-minute washout in Ames/candesartan (six cells, five animals).

For live cell analysis, microglial images were collected at the inner plexiform layer (IPL), and custom written macros using ImageJ 1.43 Freeware (National Institutes of Health, Bethesda, MD, USA) were utilized. Microglial changes in retinal explants were assessed from maximum intensity projections in the z-dimension and aligned in the time dimension to yield 30-minute time-lapse movies. The total microglial area as well as the average process length of microglia in each z-stack over time was calculated.

Intravitreal Injections

Adult $Cx3cr1^{+/eGFP}$ mice ($n = 27$ in total) were anaesthetized using a mixture of ketamine (67 mg/kg) and xylazine (13 mg/kg) and the ocular surface further anaesthetized with topical proxymetacaine (Alcaine, 0.5%; Alcon Laboratories, Frenchs Forest, NSW, Australia). Following dilation of the pupil with 0.5% tropicamide (Mydriacyl; Alcon Laboratories) and 10% phenylephrine hydrochloride (Minims Eye Drops; Bausch & Lomb, Macquarie Park, NSW, Australia), single intravitreal injections were made 1 mm posterior to the limbus using a 31-G needle attached to a 10-μL Hamilton syringe. Mice received 1-μL injections of 10 mM AngII (Sigma-Aldrich Corp., final concentration at retina given a 5-μL vitreal volume of 2 mM[30]), with the fellow eye receiving a 1-μL injection of vehicle control (phosphate-buffered saline [PBS]). Directly after intravitreal injection, fluorescein angiography was conducted on a subset of mice ($n = 3$) to assess changes in blood vessel caliber in response to AngII. Mice received a 100-μL intraperitoneal injection of 0.2% sodium fluorescein (Alcon Laboratories), and the retinal fundi imaged with a Micron III retinal imaging system (Phoenix Research Laboratories, Pleasanton, CA, USA) for 20 minutes as previously described.[31] Fundus images were collected and processed using the Micron III software (Stream-Pix 5.0; NorPix, Inc., Quebec, Canada).

Flow Cytometry

Twenty-four hours after injection of AngII or PBS, a subset of $Cx3cr1^{+/eGFP}$ mice ($n = 9$) were anaesthetized as described above and euthanized by cervical dislocation. Retinae and vitreous were dissected from the eyecup, pooled in groups of three retinae according to either PBS or AngII injection, and

placed into 4 mL HEPES buffered saline (137 mM NaCl, 2.5 mM KCl, 10 mM HEPES, pH 7.4, 28 mM glucose, 1.25 mM $NaH_2PO_4.H_2O$, 1 mM $MgCl_2$-$6H_2O$, 2 mM $CaCl_2$) before being dissociated (neural dissociation kit for postnatal neurons; Miltenyi Biotec). The resulting single cell suspension was incubated with a CD45-APC antibody (1:10; catalog #130-102-783, Miltenyi Biotec) to label microglia/monocytes for 15 minutes before being washed in HEPES-buffered saline (140 mM NaCl, 5 mM NaOH, 3.5 mM KCl, and 10 mM HEPES, pH 7.5, plus 5 mM glucose and 0.1% bovine serum albumin [BSA] with 0.1 mM $CaCl_2$) and passed through a 40-μm cell strainer (BD Biosciences, San Jose, CA, USA). Right Reference Standard Fluorescein High beads (Polysciences, Warrington, PA, USA) were used to calibrate the flow cytometer daily (FACSCalibur flow cytometer; BD Biosciences). Flow cytometry was used to assess baseline fluorescence in the far red (CD45) and green (eGFP) channels for each sample to quantify changes in the monocyte/microglia receptor expression in response to AngII. While both monocytes and microglia contain the fractalkine receptor Cx3cr1 and thus express eGFP in this model, peripheral monocytes display a higher intensity of the marker CD45.[32]

Immunohistochemistry

Twenty-four hours after injection of AngII or PBS, eyes of mice ($n = 15$) were collected for immunohistochemistry to assess morphology of the retina using previously described techniques.[33] The posterior eye cups of C57bl6J and Cx3cr1[+/eGFP] mice were fixed for 30 minutes in 4% paraformaldehyde in 0.1 M phosphate buffer (PB), washed three times in PB, and cryoprotected in a series of graded sucrose solutions (10%, 20%, and 30% in PB). Tissues were then either processed for flat mount immunohistochemistry, or embedded in optimal cutting temperature (OCT; Tissue-Tek OCT compound; Sakura, Torrance, CA, USA) frozen and sectioned transversely at 14 μm on a cryostat at -20°C (Microm, Walldorf, Germany). Sections were collected on poly-L-lysine coated slides (Menzel-Glaser, Braunschweig, Germany) and stored at -20°C.

For immunolabeling, slides were defrosted, washed in PB and coated in a blocking solution (10% normal goat serum [NGS], 1% BSA, 0.5% Triton-X in PB) for 1 hour. Slides were incubated overnight at room temperature in an antibody buffer (3% NGS, 1% BSA, 0.5% Triton-X in PB) containing the respective primary antibodies. Primary antibodies were used to label the AT1-R (1:100; catalog #sc-365493; Santa Cruz Biotechnology, Santa Cruz, CA, USA), Müller cells (glutamine synthetase [GS] 1:1000; catalog #MAB302; Chemicon, Bayswater, Australia), and Müller cell reactivity (glial fibrillary acidic protein [GFAP]; 1:10,000; catalog #Z0334; Dako, North Sydney, NSW, Australia). After washing in PB, sections were incubated with secondary antibody: goat anti-guinea pig, goat anti-mouse, or goat anti-rabbit conjugated to fluorescent dyes (AlexaFluor 488; catalog #A-11034 or AlexaFluor 594 catalog #A-11032; diluted 1:500; ThermoFisher Scientific, VIC, Australia) as required for 90 minutes. The sections were finally washed in PB, coated in a glycerol/Mowiol-based mounting media, and cover-slipped.

For labeling of whole retinae, entire eyecups in 30% sucrose were frozen and thawed three times, washed in PB, and blocked for 1 hour using the blocking solution (above). Retinae were then incubated for 4 days in rhodamine-conjugated peanut agglutinin (PNA) to label cone photoreceptor outer segments and terminals (1:250, #RL-1072; Vector Laboratories, Inc., Waterford, QLD, Australia) and guinea pig anti-Vesicular Glutamate Transporter 1 (VGLUT) to label bipolar cell terminals (1:1000; #AB5905, Millipore Corporation, Bayswater, VIC, Australia) dissolved in antibody buffer (above). After

washing in PB, retinae incubated in VGLUT were washed and further incubated with secondary antibody guinea pig conjugated to 594 nm overnight (diluted 1:500; Invitrogen, Carlsbad, CA, USA). All retinas were then washed in PB, coated in a glycerol/Mowiol-based mounting media, and cover-slipped photoreceptor cell–layer side up.

Retinae were imaged using a confocal microscope (Zeiss Pascal LSM-5; Carl Zeiss, Oberkochen, Germany) using an oil 40× objective. Fluorophore-labeled sections were captured at a resolution of 1024 × 1024 pixels using image browser software (Zen; Carl Zeiss) and an appropriate fluorescence filter (Alexa 594/CY3: excitation 568 nm, emission filter 605/32; Alexa 488/FITC: excitation 488 nm, emission filter 522/32; ThermoFisher Scientific). Red, green, and blue fluorescence were scanned separately and adjusted for black levels and contrast with graphics editing software (Photoshop CS6; Adobe Systems, San Jose, CA, USA).

For fixed cell morphologic analysis following intravitreal injection, at least three high resolution Z-stack images containing four to six microglia per image were captured using a ×40 oil objective (0.7× zoom) for each retinae. Microglial morphology was assessed using the software, MetaMorph Offline (Molecular Devices Corporation, Sunnyvale, CA, USA). For analysis of microglial interaction with photoreceptor and bipolar cells, cell terminals were labeled with either PNA or VGLUT1, and the percentage of terminals overlapping with microglial cells in either the outer plexiform layer (OPL; photoreceptor, PNA) or IPL (bipolar, VGLUT1) was analyzed between treated and contralateral control eye using MetaMorph.

RNA Isolation and Quantitative PCR Gene Array

Retinae from Cx3cr1[+/eGFP] mouse eyes ($n = 9$ each group) were dissected from the posterior eyecup as described for flow cytometry 24 hours after AngII, PBS, or candesartan + AngII or PBS intravitreal injection. Methods for RNA isolation and quantitative PCR have been published previously.[34] Briefly, total RNA was isolated using commercial spin columns (RNeasy; Qiagen), retinal RNA samples (each 25 ng) were pooled into respective treatment groups (three independent experiments each containing three pooled samples), and reverse transcribed (RT[2] first strand; Qiagen). A quantitative PCR gene array was used to assess the expression of 84 cytokine and chemokine genes involved in the immune response and other pathways (Cytokines & Chemokines RT[2] Profiler PCR Array; Qiagen). The samples were added to the commercial master mix (RT[2] SYBR Green Master Mix; Qiagen) and amplified for 40 cycles (ABI 7900HT; Life Technologies, Grand Island, NY, USA). Three independent arrays were performed for each treatment group. The data were analyzed using $\Delta\Delta$Ct, expressed as a fold change and regulation assessed using an unpaired t-test.

Statistical Analysis

Statistical analysis was performed with GraphPad 7 Prism Software (GraphPad Software, Inc., San Diego, CA, USA). Results are expressed as the mean ± SEM. Multiple group comparisons for live cell imaging of retinal explants were performed with a 2-way ANOVA for time and drug treatment, and a Tukey's post hoc test was utilized to make individual comparisons between treatments as appropriate. Statistical significance is indicated by * for $P < 0.05$. Microglial morphology and number comparisons between saline and AngII injected eyes were made with a Student's t-test and statistical significance indicated by * for $P < 0.05$. The Mann-
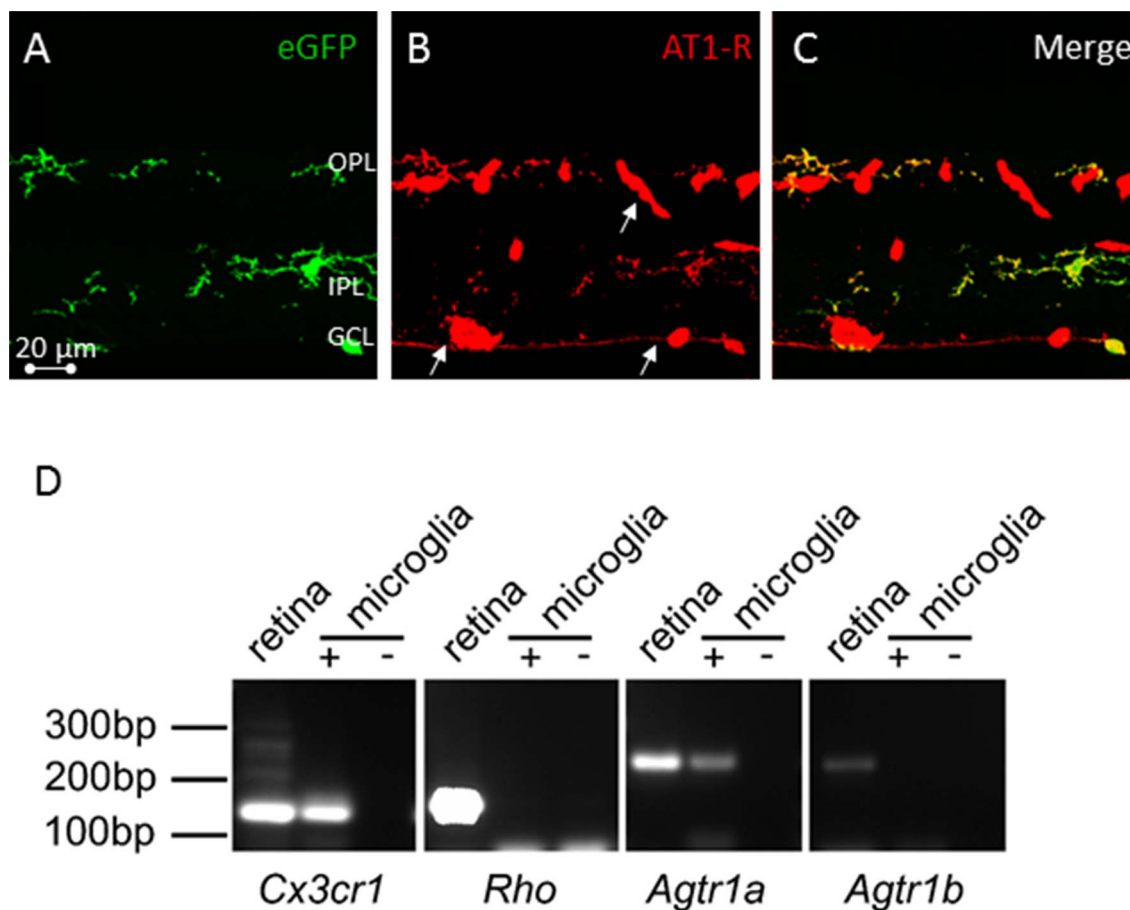
FIGURE 1. The AT1-R is expressed by retinal microglia. (**A–C**) Vertical cryostat sections from 3-month-old Cx3cr1[+/eGFP] showing (**A**) *green* eGFP staining of retinal microglia, (**B**) *red* AT1-R staining of microglia and blood vessels (*arrows*), and (**C**) co-localization of microglia and AT1-R. (**D**) Isolated microglial samples were shown to express the microglial gene *Cx3cr1*, while *Rho* expression was only evident in the total retinal samples. The *Agtr1a* gene product was expressed in the microglial samples while the *Agtr1b* isoform was not present. Retina = total retinal sample. Microglia + = FACS isolated microglial sample. Microglia − = FACS isolated microglial RNA in the absence of reverse transcriptase.

Whitney rank sum test was used when nonparametric statistics were required.

RESULTS

Retinal Microglia Express the AT1 Receptor

Microglia from Cx3cr1[+/eGFP] retinae displayed typical ramified morphology,[2] with their cell bodies restricted to the plexiform layers of the retina while their processes extended and branched throughout the retina (Fig. 1A). AT1-R immunolabeling was observed on retinal vessels (see arrows) as previously reported,[21] as well as being expressed on the processes and soma of microglia in the IPL and OPL (Fig. 1B). eGFP expression was co-localized with AT1-R immunolabeling in all microglia cells (yellow) observed in the OPL, IPL, and GCL (Fig. 1C). In order to validate this result, we isolated retinal microglia using FACS, and performed RT-PCR. The purity of the microglial sample was assessed by amplifying microglial-specific (*Cx3cr1*) and photoreceptor (*Rho*) genes. While *Cx3cr1* amplified products were observed in both the retinal and microglial samples, the *Rho* was only found in the total retinal samples (Fig. 1D). Respective negative controls (microglial RNA in the absence of reverse transcriptase) showed no presence of genomic contamination. With respect to AT1-R expression, a product corresponding to *Agtr1a* was

evident in both the microglial-isolated and retinal sample, while the *Agtr1b* gene product was only expressed in the total retinal sample. Agtr1a and Agtr1b represent different isoforms of the AT1R, with Agtr1a being more highly expressed in most tissues.[35] The absence of either isoform can be compensated for by the presence of the other, suggesting similar functions.[36] Hence, it is likely that the dominant isoform in the retina is Agtr1a, and explains the presence of this isoform only on our isolated microglial sample. Thus, retinal microglia express the AT1 receptor and therefore have the capacity to be modulated by AngII.

Microglial Morphology Is Altered by AngII in Living Tissue and Ameliorated by AT1-R Blockade

To study whether microglial behavior was altered by AngII, retinal wholemounts from 5- to 8-week-old Cx3cr1[+/eGFP] mice were isolated and retinal microglia imaged using time-lapse confocal microscopy. Retinal explants were maintained in a temperature controlled chamber through which 37°C carbogenated Ames solution was constantly perfused. Time-lapse confocal microscopy over 30 minutes showed microglia had dynamic processes that changed in shape and length over time, while their soma remained relatively stable (Fig. 2A; Supplementary Movie S1). Similar microglial movements have previously been reported in the retina.[2] The addition of AngII to the perfusate resulted in a rapid retraction of processes and
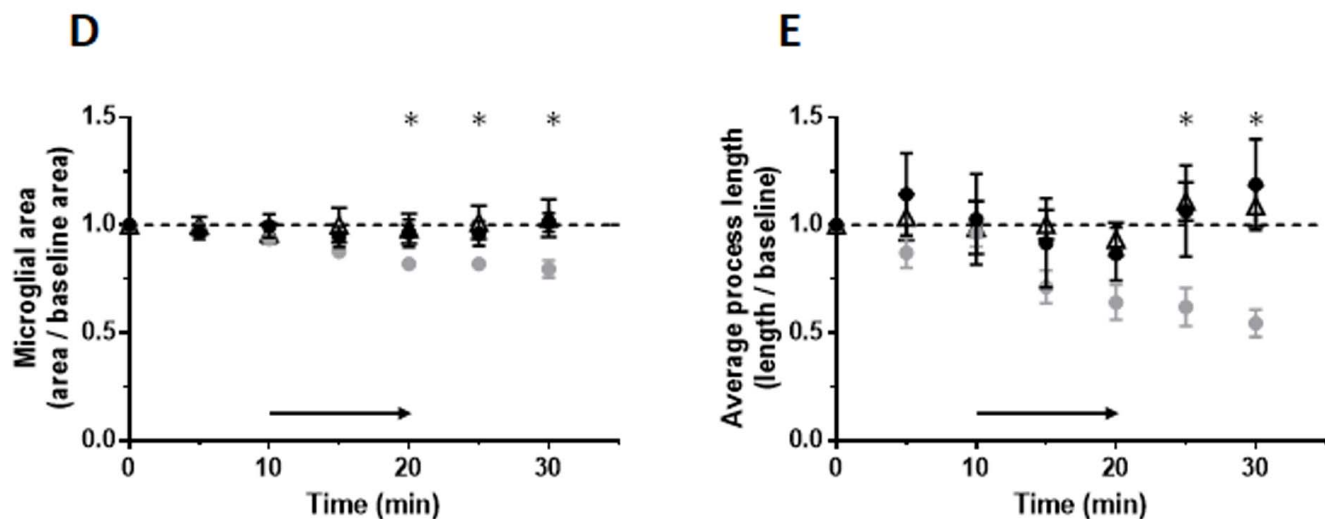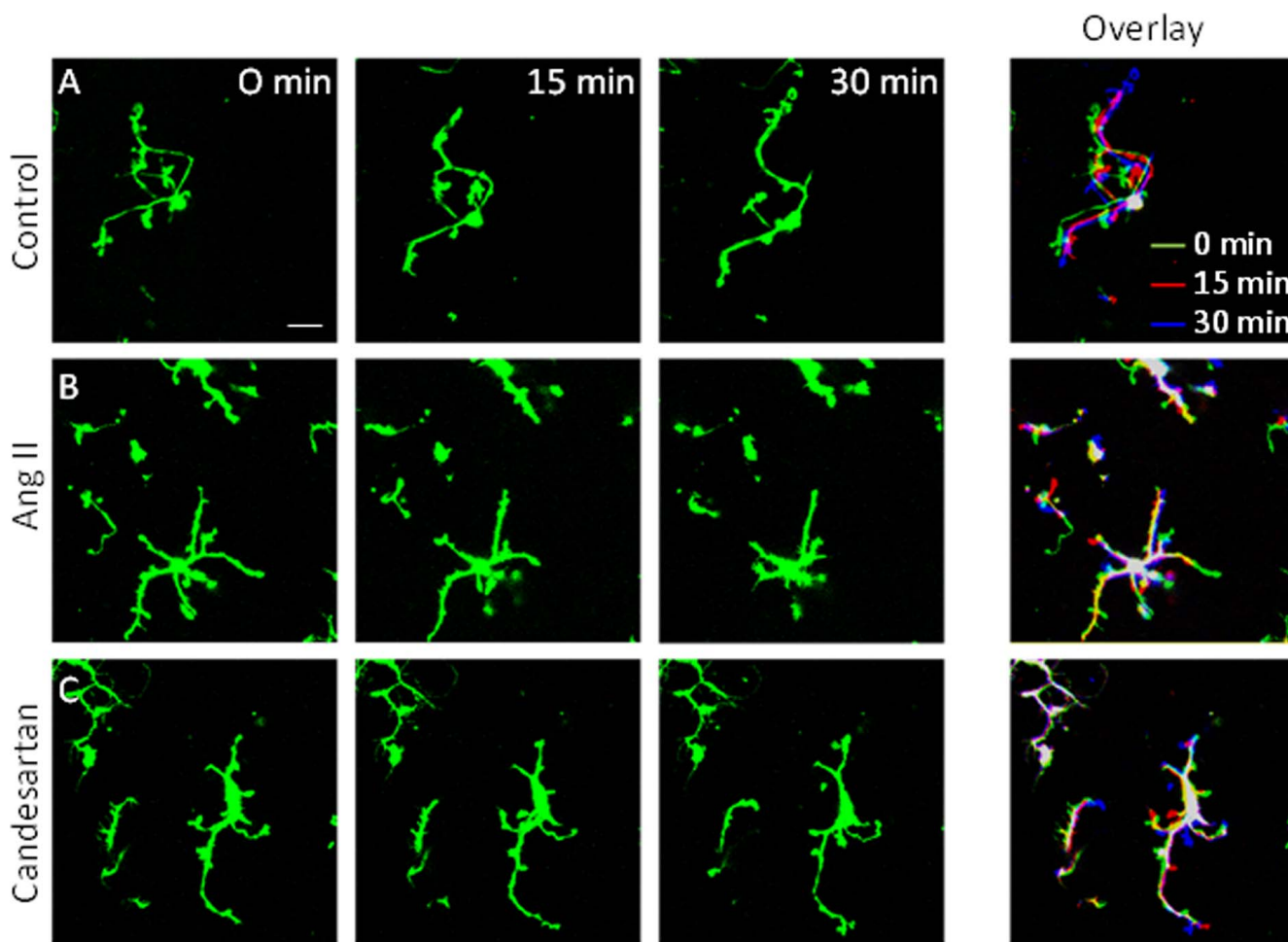
FIGURE 2. Retinal microglial dynamics are altered by AngII and the changes prevented by AT1-R blockade with candesartan. (**A**) Microglia under control conditions with constant perfusion by carbogenated Ames display retracting and expanding processes over time with a stable cell soma (overlay). (**B**) Perfusion with 5 μm AngII produces an immediate activation of microglia with retraction of processes and a total decrease in microglial area over time. (**C**) Preincubation of retinal explants with 0.1 μg/mL candesartan followed by perfusion of 5 μm AngII showed no change in total microglia area over time, with microglia displaying similar retracting and expanding processes with stable cell soma as seen in the control condition. *Scale bar*: 30 μm. Quantification of total microglial area (**D**) and average process length (**E**) relative to baseline under control (*black circles*, $n = 7$), AngII perfusion (*gray circles*, $n = 8$), and candesartan treated (*white triangles*, $n = 6$) conditions showed AngII exposure resulted in significantly decreased microglial area and process length. This was abolished with candesartan preincubation. *Dotted line* indicates baseline area for control cells. AngII perfusion occurred between 10 and 20 minutes post recording (*arrow*). Data presented as mean ± SEM, *$P < 0.05$.
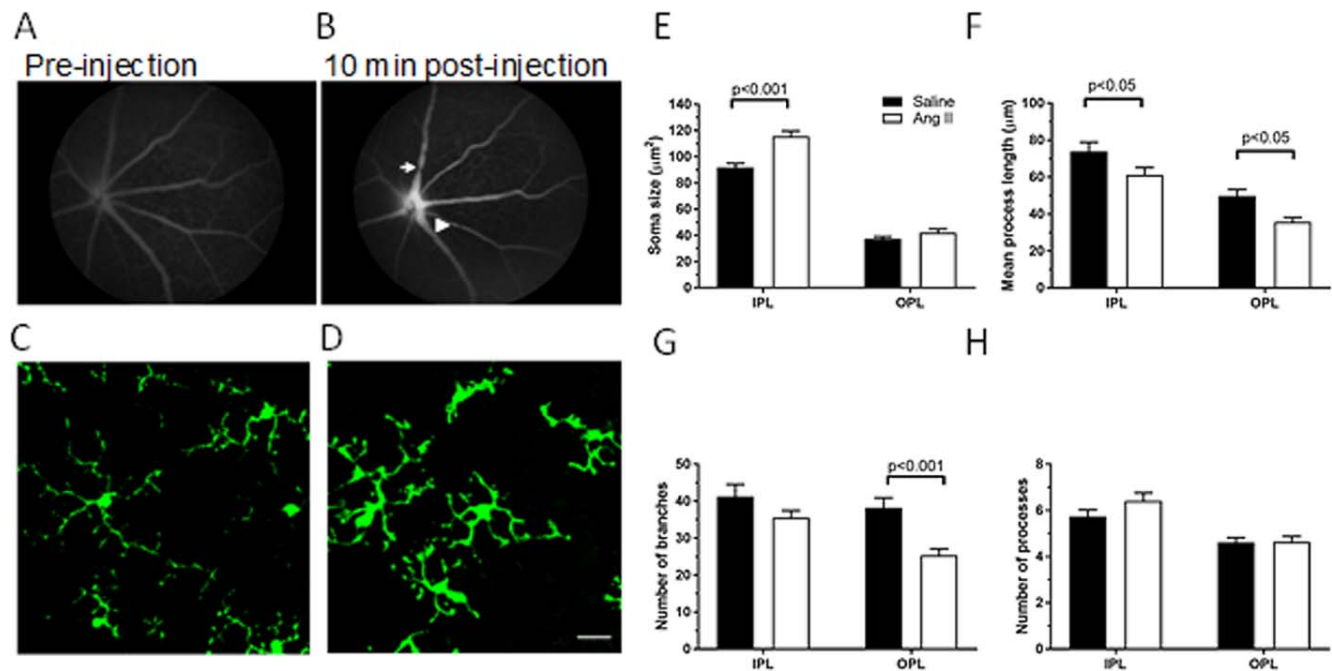
FIGURE 3. AngII causes activation of microglia 24 hours following injection into the eye. (A, B) Fundus images before (A) and after (B) fluorescein injection showing constriction of blood vessels (arrowhead) and vascular beading (arrow) 10 minutes following intravitreal injection of 10 mM AngII into the eye. (C, D) Representative fixed retinal wholemounts of eGFP expressing microglia 24 hours following either (C) PBS or (D) 10 mM AngII injection into the eye. (E–H) Quantification of microglial activation state for PBS ($n = 5$) and AngII injected ($n = 5$) eyes. AngII injected eyes showed significantly increased soma size (E, $P < 0.001$) in the IPL and significantly decreased process lengths (F, $P < 0.05$) compared to PBS control eyes in the IPL and OPL. A significant decrease in the number of branches in the processes was also seen in the OPL (G, $P < 0.001$). Data are presented as mean ± SEM.

an apparent increase in soma size (Fig. 2B; Supplementary Movie S2). This was abolished when retinae were preincubated with the AT1 receptor antagonist, candesartan, with microglia exhibiting similar process movement and soma stability to control incubations (Fig. 2C; Supplementary Movie S3). When the AngII-dependent effects were quantified, a decrease in both total microglial area (Fig. 2D, gray circles; −14.3%, $P < 0.05$) and mean process length (Fig. 2E, gray circles; −42%, $P < 0.05$) was evident compared to Ames alone (black circles). Both effects were evident for the remainder of the recording period (30 minutes postbaseline, total area −21.5%, $P < 0.05$; mean process length −41%, $P < 0.05$). Blockade of AT1-R with candesartan ameliorated the effects of AngII perfusion on both total microglial area (Fig. 2D, open triangles) and mean process length (Fig. 2E, open triangles), with neither measure significantly different from control. These results suggest AngII has a direct action on retinal microglia via the AT1-R that causes a phenotypic change similar to microglial activation.

AngII Causes Sustained Activation of Microglia

In order to further examine the effect of AngII on retinal microglia in vivo, intravitreal injections of either AngII or PBS were performed. In order to validate the retinal bioavailability of AngII following injection, its vasoactive effect was assessed in vivo using fluorescein angiography (Figs. 3A, 3B). Figure 3B shows that delivery of AngII into the vitreous had a rapid effect on retinal vessels, with constriction and beading of blood vessels observed 10 minutes postinjection (see arrows), consistent with previous reports.[16] Having shown the exogenous AngII was active in vivo, we subsequently explored the effect of AngII on retinal microglia using immunohistochemistry 24 hours posttreatment. Retinal flatmounts were imaged at the level of both the IPLs and OPLs in order to assess

microglial morphology. While the microglia in PBS treated eyes appeared normal (Fig. 3C), AngII treated eyes showed an increase in microglial soma size and a decrease in process length at the level of the IPL (Fig. 3D). Similar results were found in the OPL. When microglial changes were quantified, AngII caused a significant increase in microglial soma area (Fig. 3E, soma size: IPL Saline 91.8 ± 3.15 μm versus AngII 115.5 ± 4.10 μm, $P < 0.05$) and decreased microglial process length (Fig. 3F, IPL Saline 73.9 ± 5.0 μm versus AngII 61.2 ± 4.02 μm, $P < 0.05$; OPL Saline 49.8 ± 3.5 μm versus AngII 35.8 ± 2.4 μm, $P < 0.05$). There was also a significant decrease in the number of branches in the OPL, consistent with the decrease in process length (Fig. 3G; OPL Saline 38.2 ± 2.7 μm versus AngII 25.3 ± 1.8 μm, $P < 0.001$). These in vivo AngII-mediated changes in microglial morphology are consistent with our in vitro explant data (Fig. 2) and reflect the morphologic change that occurs following microglial activation.[37]

AngII Causes an Increase in Inflammatory Chemokines and Cytokines

Microglial activation is known to result in the production of inflammatory cytokines and chemokines. We examined the effect of AngII on the expression of retinal inflammatory mediators by using a commercial PCR array to screen 84 cytokine/chemokine-related genes. The intravitreal delivery of AngII significantly altered the expression of 18 genes (t-test $P < 0.05$), with the majority showing increased expression, while only Ctf1 and Hc were downregulated (Table). Of the 18 regulated genes, 15 showed a greater than twofold change, with Cxcl1 and Il6 expression increased by 11.9- and 10.4-fold, respectively (Fig. 4). Several of these genes are involved in Ccr and Cxcr chemokine receptor binding signaling pathways, and include several proinflammatory cytokines (Il-1b, Il-6, Lif,

TABLE. Gene Ontology (GO) Analysis of the Cytokine/Chemokine Array Showing AngII Regulated Genes

Panther Pathways	Mus Musculus (REF)	Gene Input	Gene Input (Expected)	Fold Enrichment	P Value	Genes
CCR2 chemokine receptor binding	4	3	0	>100	1.70E-05	Ccl2, Ccl12, Ccl7
CCR chemokine receptor binding	32	7	0.03	>100	1.89E-12	Ccl2, Ccl3, Ccl7, Ccl11, Ccl12, Ccl17, Ccl22
Leukemia inhibitory factor receptor binding	3	2	0	>100	9.42E-03	Lif, Ctf1, OSM
CXCR chemokine receptor binding	13	3	0.01	>100	5.80E-04	Cxcl1, Cxcl10, Cxcl12

Osm). Preinjection of candesartan prior to AngII blocked the increases in these proinflammatory cytokines (Supplementary Fig. S1). Overall these data suggest that delivery of AngII results in an overall proinflammatory environment within the retina.

AngII Causes an Increase in the Peripheral Monocyte Population Within the Retina

As microglial activation can often be coincident with an increase in macrophage/monocyte number, we examined the changes to specific macrophage populations caused by AngII by using immunocytochemistry and flow cytometry with specific antibodies to separate retinal microglia from peripheral monocytes. Microglia can be differentiated from peripheral monocytes, both of which contain the fractalkine receptor Cx3cr1, by the relative intensity of expression of the marker CD45 (microglia, eGFP/CD45^{low}; peripheral monocytes eGFP/CD45^{high}).[32,38] Figures 5A through 5D show representative images from eyes injected with either PBS (Figs. 5A, 5C) or AngII (Figs. 5B, 5D) and the location of CD45-APC and GFP$^+$ cells in these retina. These images show an increase in the population of CD45-APC cells in both the retina, vitreous and surrounding tissues in AngII injected eyes (Fig. 5B), particularly in the peripheral retina (Fig. 5D). These results were further investigated using flow cytometry (Figs. 5E–G), where retina from PBS and AngII-treated eyes were each characterized by two separate populations of CD45/GFP expressing cells. The fluorescent dot plots for PBS (Fig. 5E) and AngII (Fig. 5F) show an altered proportion of cells characterized as CD45^{high}. When quantified, there was a significant increase in the total number of GFP$^+$/CD45$^+$ cells in AngII-treated eyes (Fig. 5G, PBS 171.7 $\pm$ 19.0 versus AngII 410.7 $\pm$ 65.1, $P < 0.05$), which was due to an increase in the number of eGFP/CD45^{high} cells (Fig. 5G; saline 18.7 $\pm$ 4.10 versus AngII 225 $\pm$ 79.0, $P < 0.05$). There was no significant difference in eGFP/CD45^{low} numbers between the two groups (saline 153.0 $\pm$ 18.1 versus AngII 185.7 $\pm$ 13.8, $P > 0.05$ ns). These data, together with the

increase in cells seen in AngII injected eyes in Figures 5B and 5D, suggest intravitreal administration of AngII induces recruitment of circulating monocytes (eGFP/CD45^{high}) to the retina.

AngII Does Not Cause Müller Cell Gliosis or Neuronal Cell Death at 24 Hours Postinjection

Since AngII can have wide-ranging tissue effects, we sought to determine whether the activation of microglia was a specific AngII effect, or indicative of a more generalized retinal effect. Müller cell gliosis is a generalized biomarker of retinal stress and is characterized by increased GFAP expression. Müller cells were imaged using the cell marker GS (green), with no overt disruption of retinal Müller cell morphology observed in either the PBS (Fig. 6A) or AngII (Fig. 6D) treated eyes. GFAP expression was restricted to the astrocytes within both treatment groups (Figs. 6B, 6E), and there was no increased GFAP expression observed in AngII-exposed Müller cells compared to control (Figs. 6C versus 6F). Moreover, when the effect of AngII on retinal neuronal cell death was investigated by TUNEL staining (red), there was no evidence of increased neuronal apoptosis in any of the cellular layers (cell nuclei, DAPI, blue) in either AngII (Fig. 6H) or PBS injected eyes (Fig. 6G). A retina from an rd1 (retinal degeneration) eye was used as a positive control for the TUNEL method, and showed clear neuronal apoptosis (Fig. 6I, TUNEL, red; DAPI, blue). This suggests the concentration of AngII injected is not directly toxic to retinal neurons and the microglial activation identified was not the result of a generalized AngII retinal effect.

Retinal Microglia Show Decreased Neuronal Contacts Following Intravitreal Injection of AngII

Microglia are known to make contacts with neurons in the normal retina, facilitating neuronal-microglial communication. In order to determine whether AngII exposure altered microglial-neuronal contact, immunohistochemistry was used to explore the OPLs and IPLs. Microglial (green) contacts with VGLUT1 positive, rod bipolar cell terminals (red) in the IPL are shown in Figures 7A (PBS) and 7C (AngII). The images were rendered (Fig. 7B, PBS; Fig. 7D, AngII) to identify those bipolar cell terminals that were contacted by microglia (red) from the remaining bipolar cell terminals (blue). In AngII injected retina, there were significantly fewer bipolar cell-microglial contacts 24 hours postinjection (Fig. 7E, $n = 4$, saline 15.6 $\pm$ 2.31 versus AngII 7.8 $\pm$ 1.06, $P < 0.05$). At the level of the OPL, microglial (green) contacts with PNA positive, cone photoreceptor terminals (red) are shown for PBS (Fig. 7F) and AngII (Fig. 7H) injected eyes. Unlike contacts in the IPL, microglial contacts with cone terminals were not significantly altered in AngII injected eyes (Fig. 5J; $n = 4$, saline 35.7 $\pm$ 4.67 versus AngII 48.5 $\pm$ 9.33).
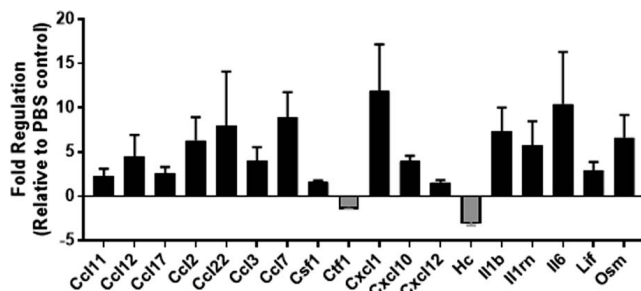

FIGURE 4. AngII causes an increase in inflammatory chemokines and cytokines. Gene expression was significantly altered ($P < 0.05$) in 18 target genes 24 hours after injection of AngII, with 16 of the 18 genes showing an increased expression. Data are represented as a change relative to PBS injected control eyes and presented as mean $\pm$ SEM, $n = 3$.
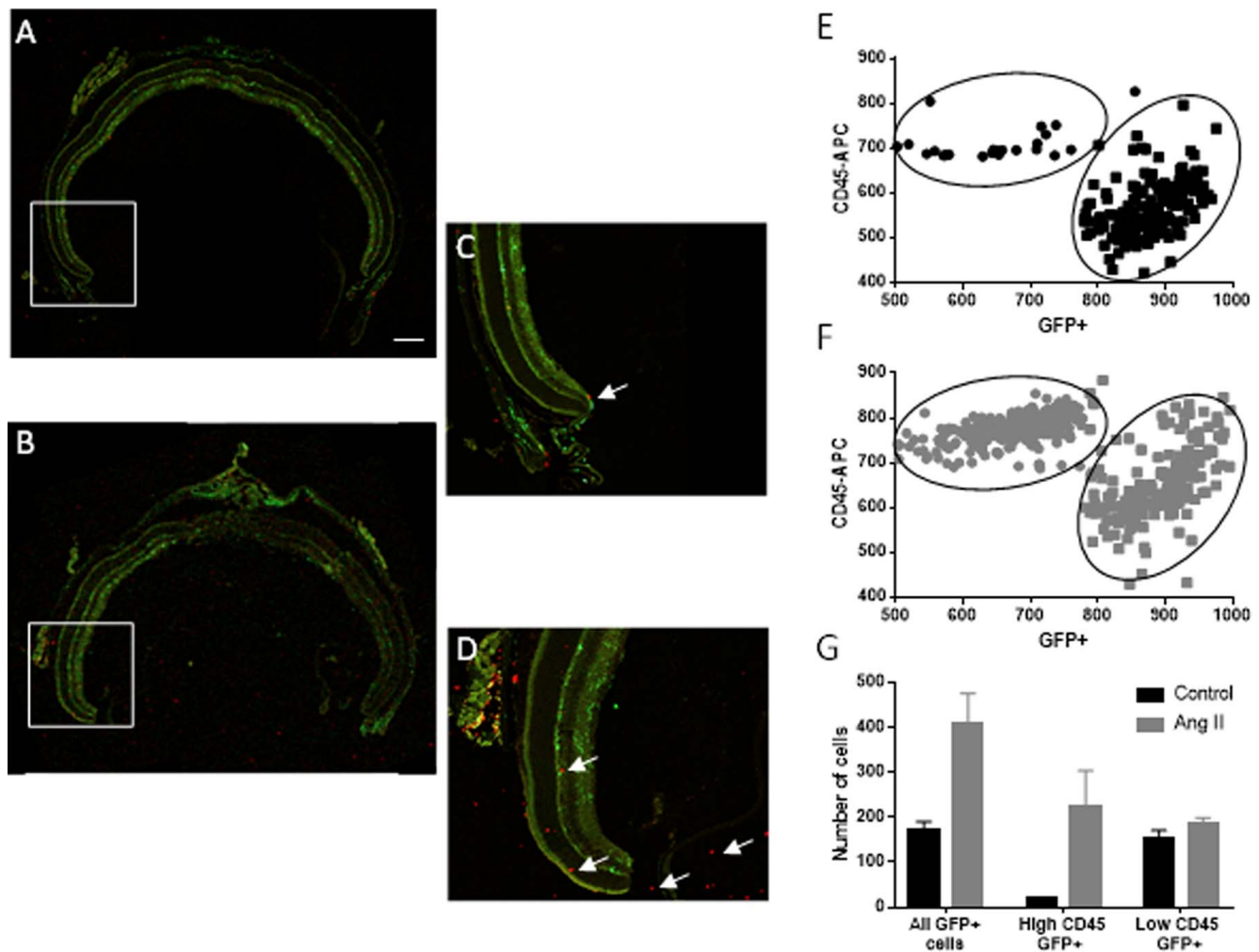
FIGURE 5. AngII causes an increase in retinal monocytes 24 hours following injection into the eye. (**A–D**) Intravitreal injection of AngII causes an increase in CD45-APC-positive cells in the retina and vitreous 24 hours after injection of AngII. Representative images of the retina from saline injected (**A**) and AngII injected (**B**) eyes. *White squares* represent magnified sections of peripheral retina and vitreous for saline (**C**) and AngII (**D**) injected eyes. *White arrows* point to examples of monocytes in the retina (**B**, **D**) and vitreous (**D**). *Scale bar*: 200 μm. (**E–G**) Flow cytometry analysis of the number of eGFP and CD45-positive cells in PBS (**E**, $n = 3$ groups) and AngII (**F**, $n = 3$ groups) injected eyes. (**G**) Quantification of the total number of cells expressing high levels of eGFP found a significant increase in AngII injected eyes ($P < 0.05$). Cells that were gated for eGFP^{high}/CD45^{low} expression showed no change in number between PBS and AngII eyes, while there was a significant increase in the number of eGFP^{high}/CD45^{high} cells in AngII compared to PBS control eyes ($P < 0.05$).

DISCUSSION

Changes in AngII/AT1-R signaling are common in many retinal diseases and in particular hypertensive and diabetic retinopathy,[16,39,40] leading directly to retinal vascular leakage and devastating visual consequences. While previous work has reported AT1-R expression on brain microglia,[26,41,42] our finding of AT1-Rs localized to microglia using fluorescence immunohistochemistry and confirmed with PCR analysis on FACS-isolated retinal microglia, is the first report of AT1-R expression localized to microglia within the retina, and has important implications for vision in diseases where increases in AngII and inflammation play an important role.

The presence of the AT1-R on microglia suggests AngII is capable of eliciting a specific microglial response. The application of AngII to live retinal explants induced a rapid change in microglial morphology that was sustained at 24 hours and was consistent with an activated phenotype. This effect was confirmed in vivo, with AngII injection resulting in a retraction of microglial processes and an increase in soma size, again

consistent with a classical activation pattern.[43] We confirmed that this activation was likely attributable to AT1-R on microglia by blocking the response with the AT1-R antagonist, candesartan. This direct action of AngII on microglia is supported by an in vitro study showing AngII facilitated LPS activation of cultured rat microglia via AT1-R activation.[44] Furthermore, previous observations from our group showed that activated microglia were present in a model of oxygen-induced retinopathy, a condition known to be associated with an increase in AngII within the vitreous, and that this activation was ameliorated by AT1-R blockade.[45] Interestingly, a previous in vitro study has indicated that retinal microglial activation is also modulated via prorenin, an upstream modulator of Angiotensin production.[25] Our results from ex vivo imaging of microglia show that the addition of candesartan to the perfusion medium causing blockade of the AT1R did not result in a change in the activation state of microglia under control conditions (first 10 minutes of recording) (Figs. 2C–E). This suggests that the presence of AT1-R on microglia is related to mediating effects in cases where there is an increase in exogenous AngII, such as in
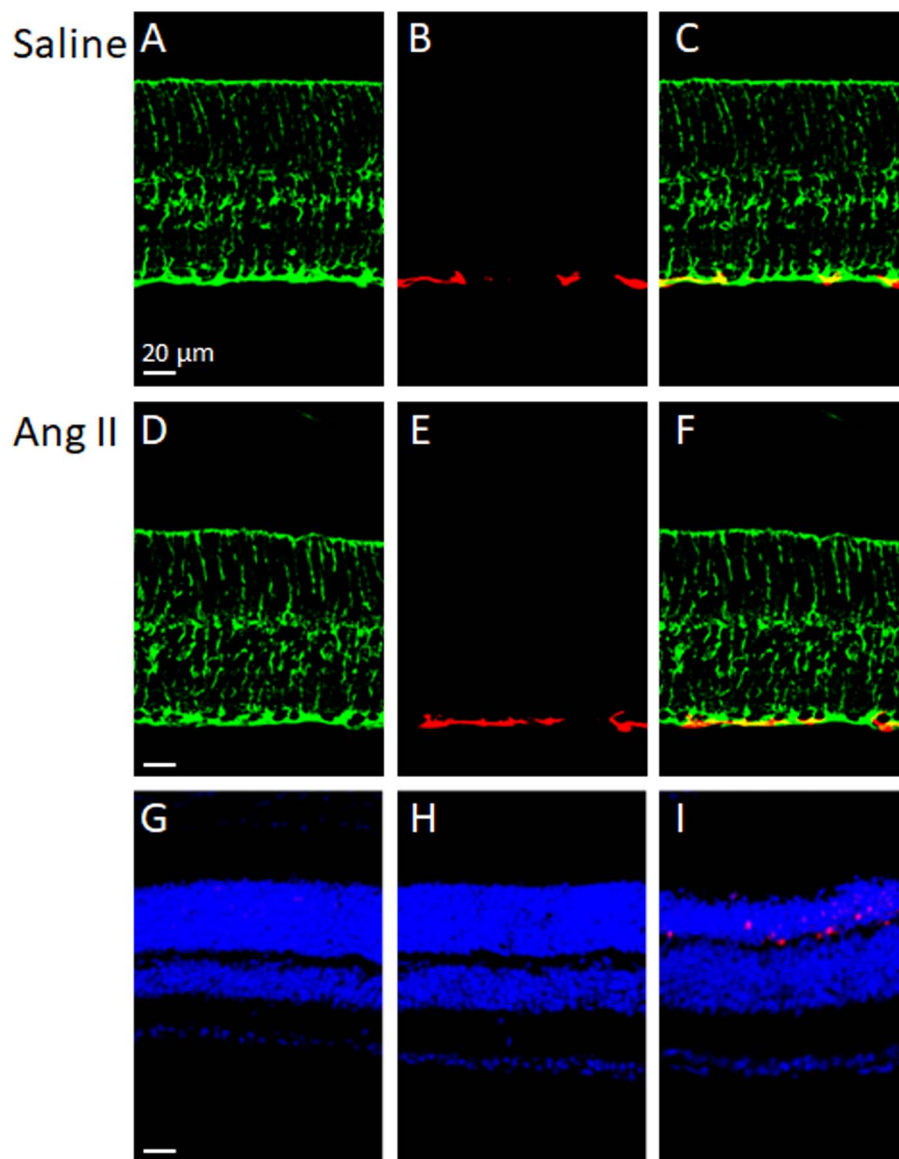
FIGURE 6. AngII does not cause Müller cell gliosis or neuronal apoptosis at 24 hours following intravitreal injection into the eye. (A–F) Representative vertical confocal micrographs showing GS staining of Müller cells (green), and GFAP staining (red) in PBS control (A–C) and AngII injected eyes (D–F). No reactive gliosis was seen in either group. (G–I) TUNEL staining (red) was assessed in PBS control (G) and AngII injected eyes (H) with nuclei counterstained with DAPI (blue). A vertical section from an Rd1 (retinal degeneration) mouse was used as a positive control (I) showing neuronal apoptosis in red. Scale bars: 20 µm. ONL, outer nuclear layer; INL, inner nuclear layer.

diabetic retinopathy, rather than in the general maintenance of microglia. Several other studies have also reported on the capacity of RAS antagonists to reduce tissue inflammation and microglial activation.[11,28] Thus the current data, in conjunction with previous work, suggest that microglial activation can be regulated by multiple constituents of the RAS.

Our data showed that AngII exposure resulted in a prolonged activation of retinal microglia, with effects evident at least 24 hours posttreatment. This sustained activation is interesting, given the short half-life (16–30 seconds) of AngII in plasma.[46,47] However, AngII in tissues such as the heart and kidney has a significantly longer half-life (15 minutes) and has also been shown to accumulate in tissues after internalization by binding to the AT1-R.[47] This is likely to be the case in retinal tissue, where AngII either injected or perfused binds to AT1-R located on retinal microglia, is subsequently internalized and causes sustained activation. While this current study did not

detail the downstream AngII-dependent activation pathways that may be involved in the sustained activation of microglia in AngII injected eyes, previous work has shown IκBα degradation, activation of the NFκB and STAT3 inflammatory pathways, in addition to increased TGF-β expression are specifically altered, and could contribute to this finding.[48,49]

The activation of microglia is known to result in the production of several proinflammatory cytokines,[50] and this activation state is confirmed by data from our PCR array showing increased proinflammatory cytokines such as *Il-1b*, *Osm*, and *Il-6* with injection of AngII. Increased *Il6* and *Lif* gene expression have been reported previously in AngII induced cardiomyocyte hypertrophy,[51] while Il-6 was shown to be critical in the retinal vascular remodeling that occurred after AngII administration.[52] Considering the role of increased AngII in inflammatory eye conditions, such as hypertensive and diabetic retinopathy,[53] the concept that AngII can activate
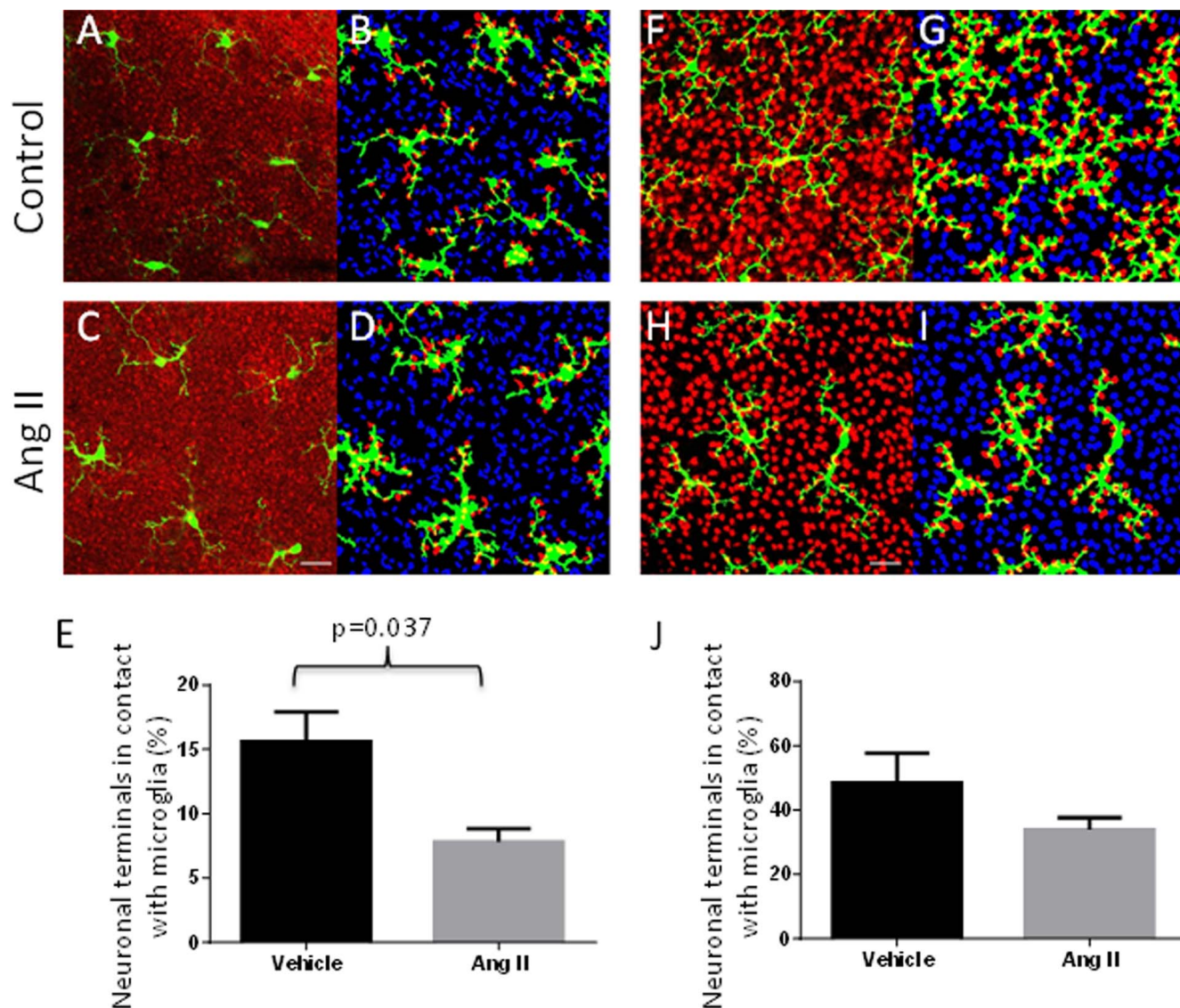
FIGURE 7. AngII causes a decrease in microglial/neuronal contacts. (A–E) The number of microglial cell processes (*green*) contacting bipolar cell terminals was assessed by immunofluorescence staining of bipolar cell terminals with VGLUT (*red*). Representative images from PBS control (A) and AngII injected eyes (C) were rendered to identify microglial-bipolar contacts (B, D, respectively). Quantification of the number of microglial contacts with bipolar cell terminals found a significant reduction in AngII injected eyes (E, *$P < 0.05$, $n = 3$). (F-J) The number of microglial cell processes (*green*) contacting cone photoreceptor cell terminals was assessed by immunofluorescence staining of photoreceptor cell terminals with PNA (*red*). Representative images from PBS control (F) and AngII injected eyes (H) were rendered to identify microglial-cone photoreceptor contacts (G, I, respectively). There was no change in the number of microglial contacts with cone photoreceptor cell terminals on quantification in AngII injected eyes (J, $n = 5$). Data shown as mean ± SEM. *Scale bars*: 20 μm.

microglia and cause increased production of inflammatory cytokines is very relevant. Moreover, this possibility agrees with the large body of evidence suggesting that AngII's effects in the retina and brain are not restricted to its direct modulation of vascular tone.[25,54,55] The presence of AT1-R on retinal microglia suggests a pathway by which the excess AngII present during retinal disease can result in microglial activation and proinflammatory cytokine/chemokine release into the retina. This is particularly important to the early retinal changes associated with diabetic retinopathy, which are known to involve increases in vitreal RAS components.[39] It should be acknowledged, however, that AT1R are known to be expressed on the retinal vasculature[21] and that vascular changes are induced by exogenous AngII (Fig. 3).[16] Hence, the changes observed in both microglia and cytokine/chemokine expression are likely to be contributed to by AngII induced vascular changes.

In addition to the increase in proinflammatory cytokines, AngII treatment led to the increase in a number of genes involved in chemokine receptor binding pathways (CCR, CCR2, CXCR; Table). These pathways are often involved in recruiting other immune cells to the affected area.[56] For example, the CCR/CCl2 chemokine receptor system has been shown to be crucial for the recruitment of peripheral monocytes to the CNS.[57] The change in this gene pathway is consistent with the significant increase in the presence of systemic monocytes (eGFP/CD45high) seen in AngII injected eyes, and has likely contributed to the increase in this system found in our whole retinal samples (Fig. 4). The increase in monocytes, which are phenotypically distinct from macrophages[58] (Figs. 5A–D), agrees with the increases in monocyte/leukocyte adhesion[40] and retinal vascular leakage[16] common in retinal diseases that are known to have increases in AngII.

AngII-mediated effects were predominantly limited to microglial activation, with no generalized retinal effect evident, as judged by Müller cell gliosis and overt neuronal apoptosis. It is known that high concentrations of ATP injected intravitreally cause photoreceptor apoptosis after 24 hours[59] and injection of NMDA causes amacrine and ganglion cell apoptosis from 1 hour post injection,[60] so it can be concluded that the concentration of AngII injected into the vitreous in our animals was not toxic to the neurons at 24 hours. There was, however, a decrease observed in the number of contacts microglia made with inner retinal neurons. This finding is consistent with the significant decrease in process length found with AngII activated microglia in the inner nuclear layer of the retina (Figs. 2, 3). Decreased microglial/neuronal interactions via activation with AngII would disturb the many roles that microglia are known to play in neuronal maintenance, including phagocytosis of neuronal debris[61] and maintaining synaptic function,[62] highlighting the complexity of AngII/AT1-R signaling in the retina. Thus, over time and with continued AngII exposure, as might occur during insult or disease, the reduced microglial-neuronal contacts may negatively impact neuronal function. Further to this, prolonged proinflammatory cytokine production may also result in neuronal dysfunction and possibly death.

We show that retinal microglia express AT1-R and that AngII causes selective activation of retinal microglia both immediately and 24 hours following injection of AngII into the eye. The results suggest that AngII may directly activate AT1-Rs on microglia to induce an activation response and the production of inflammatory factors. This pathway may be critical in the normal response of microglia to retinal injury or infection. Furthermore, in retinal diseases such as diabetic retinopathy, where there is an increase in AngII, the presence of AT1-Rs on microglia may lead to increased microglial activation and inflammatory responses that could exacerbate the disease. Targeting this activation pathway in diseases such as diabetic retinopathy may prove useful in limiting pathology.

References

1. Hanisch UK, Kettenmann H. Microglia: active sensor and versatile effector cells in the normal and pathologic brain. *Nat Neurosci*. 2007;10:1387–1394.

2. Lee JE, Liang KJ, Fariss RN, Wong WT. Ex vivo dynamic imaging of retinal microglia using time-lapse confocal microscopy. *Invest Ophthalmol Vis Sci*. 2008;49:4169–4176.

3. Nimmerjahn A, Kirchhoff F, Helmchen F. Resting microglial cells are highly dynamic surveillants of brain parenchyma in vivo. *Science*. 2005;308:1314–1318.

4. Du L, Zhang Y, Chen Y, Zhu J, Yang Y, Zhang HL. Role of microglia in neurological disorders and their potentials as a therapeutic target. *Mol Neurobiol*. 2017;54:7567–7584.

5. Davies DS, Ma J, Jegathees T, Goldsbury AC. Microglia show altered morphology and reduced arborisation in human brain during aging and Alzheimer's disease. *Brain Pathol*. 2017;27:795–808.

6. Melief J, Schuurman KG, van de Garde MD, et al. Microglia in normal appearing white matter of multiple sclerosis are alerted but immunosuppressed. *Glia*. 2013;61:1848–1861.

7. Miron VE, Boyd A, Zhao JW, et al. M2 microglia and macrophages drive oligodendrocyte differentiation during CNS remyelination. *Nat Neurosci*. 2013;16:1211–1218.

8. Xu H, Chen M, Forrester JV. Para-inflammation in the aging retina. *Prog Retin Eye Res*. 2009;28:348–368.

9. Ma W, Wong WT. Aging changes in retinal microglia and their relevance to age-related retinal disease. *Adv Exp Med Biol*. 2016;854:73–78.

10. Yun JH, Park SW, Kim KJ, et al. Endothelial STAT3 activation increases vascular leakage through downregulating tight junction proteins: implications for diabetic retinopathy. *J Cell Physiol*. 2017;232:1123–1134.

11. Sun H, Wu H, Yu X, et al. Angiotensin II and its receptor in activated microglia enhanced neuronal loss and cognitive impairment following pilocarpine-induced status epilepticus. *Mol Cell Neurosci*. 2015;65:58–67.

12. Paul M, Poyan Mehr A, Kreutz R. Physiology of local renin-angiotensin systems. *Physiol Rev*. 2006;86:747–803.

13. Moravski CJ, Kelly DJ, Cooper ME, et al. Retinal neovascularization is prevented by blockade of the renin-angiotensin system. *Hypertension*. 2000;36:1099–1104.

14. Fletcher EL, Phipps JA, Ward MM, Vessey KA, Wilkinson-Berka JL. The renin-angiotensin system in retinal health and disease: its influence on neurons, glia and the vasculature. *Prog Retin Eye Res*. 2010;29:284–311.

15. Kawamura H, Kobayashi M, Li Q, et al. Effects of angiotensin II on the pericyte-containing microvasculature of the rat retina. *J Physiol*. 2004;561:671–683.

16. Phipps JA, Clermont AC, Sinha S, Chilcote TJ, Bursell SE, Feener EP. Plasma kallikrein mediates angiotensin II type 1 receptor-stimulated retinal vascular permeability. *Hypertension*. 2009;53:175–181.

17. Nadal JA, Scicli GM, Carbini LA, Nussbaum JJ, Scicli AG. Angiotensin II and retinal pericytes migration. *Biochem Biophys Res Commun*. 1999;266:382–385.

18. Nadal JA, Scicli GM, Carbini LA, Scicli AG. Angiotensin II stimulates migration of retinal microvascular pericytes: involvement of TGF-beta and PDGF-BB. *Am J Physiol*. 2002;282:H739–H748.

19. Otani A, Takagi H, Suzuma K, Honda Y. Angiotensin II potentiates vascular endothelial growth factor-induced angiogenic activity in retinal microcapillary endothelial cells. *Circ Res*. 1998;82:619–628.

20. Danser AH, Derkx FH, Admiraal PJ, Deinum J, de Jong PT, Schalekamp MA. Angiotensin levels in the eye. *Invest Ophthalmol Vis Sci*. 1994;35:1008–1018.

21. Downie LE, Vessey K, Miller A, et al. Neuronal and glial cell expression of angiotensin II type 1 (AT1) and type 2 (AT2) receptors in the rat retina. *Neuroscience*. 2009;161:195–213.

22. Danser AH, van den Dorpel MA, Deinum J, et al. Renin, prorenin, and immunoreactive renin in vitreous fluid from eyes with and without diabetic retinopathy. *J Clin Endocrinol Metab*. 1989;68:160–167.

23. Shen XZ, Li Y, Li L, et al. Microglia participate in neurogenic regulation of hypertension. *Hypertension*. 2015;66:309–316.

24. Jun JY, Zubcevic J, Qi Y, et al. Brain-mediated dysregulation of the bone marrow activity in angiotensin II-induced hypertension. *Hypertension*. 2012;60:1316–1323.

25. Shi P, Grobe JL, Desland FA, et al. Direct pro-inflammatory effects of prorenin on microglia. *PLoS One*. 2014;9:e92937.

26. Biancardi VC, Stranahan AM, Krause EG, de Kloet AD, Stern JE. Cross talk between AT1 receptors and Toll-like receptor 4 in microglia contributes to angiotensin II-derived ROS

production in the hypothalamic paraventricular nucleus. *Am J Physiol*. 2016;310:H404–H415.

27. An J, Nakajima T, Kuba K, Kimura A. Losartan inhibits LPS-induced inflammatory signaling through a PPARgamma-dependent mechanism in human THP-1 macrophages. *Hypertens Res*. 2010;33:831–835.

28. Benicky J, Sanchez-Lemus E, Honda M, et al. Angiotensin II AT1 receptor blockade ameliorates brain inflammation. *Neuropsychopharmacology*. 2011;36:857–870.

29. Jung S, Aliberti J, Graemmel P, et al. Analysis of fractalkine receptor CX(3)CR1 function by targeted deletion and green fluorescent protein reporter gene insertion. *Mol Cell Biol*. 2000;20:4106–4114.

30. Remtulla S, Hallett PE. A schematic eye for the mouse, and comparisons with the rat. *Vision Res*. 1985;25:21–31.

31. Vessey KA, Greferath U, Jobling AI, et al. Ccl2/Cx3cr1 knockout mice have inner retinal dysfunction but are not an accelerated model of AMD. *Invest Ophthalmol Vis Sci*. 2012;53:7833–7846.

32. Sedgwick JD, Schwender S, Imrich H, Dorries R, Butcher GW, ter Meulen V. Isolation and direct characterization of resident microglial cells from the normal and inflamed central nervous system. *Proc Natl Acad Sci U S A*. 1991;88:7438–7442.

33. Vessey KA, Fletcher EL. Rod and cone pathway signalling is altered in the P2X7 receptor knock out mouse. *PLoS One*. 2012;7:e29990.

34. Jobling AI, Guymer RH, Vessey KA, et al. Nanosecond laser therapy reverses pathologic and molecular changes in age-related macular degeneration without retinal damage. *FASEB J*. 2015;29:696–710.

35. Gasc JM, Shanmugam S, Sibony M, Corvol P. Tissue-specific expression of type 1 angiotensin II receptor subtypes. An in situ hybridization study. *Hypertension*. 1994;24:531–537.

36. Oliverio MI, Kim HS, Ito M, et al. Reduced growth, abnormal kidney structure, and type 2 (AT2) angiotensin receptor-mediated blood pressure regulation in mice lacking both AT1A and AT1B receptors for angiotensin II. *Proc Natl Acad Sci U S A*. 1998;95:15496–15501.

37. Stence N, Waite M, Dailey ME. Dynamics of microglial activation: a confocal time-lapse analysis in hippocampal slices. *Glia*. 2001;33:256–266.

38. Gabrusiewicz K, Ellert-Miklaszewska A, Lipko M, Sielska M, Frankowska M, Kaminska B. Characteristics of the alternative phenotype of microglia/macrophages and its modulation in experimental gliomas. *PLoS One*. 2011;6:e23902.

39. Gao BB, Chen X, Timothy N, Aiello LP, Feener EP. Characterization of the vitreous proteome in diabetes without diabetic retinopathy and diabetes with proliferative diabetic retinopathy. *J Proteome Res*. 2008;7:2516–2525.

40. Miller AG, Tan G, Binger KJ, et al. Candesartan attenuates diabetic retinal vascular pathology by restoring glyoxalase-I function. *Diabetes*. 2010;59:3208–3215.

41. Garrido-Gil P, Valenzuela R, Villar-Cheda B, Lanciego JL, Labandeira-Garcia JL. Expression of angiotensinogen and receptors for angiotensin and prorenin in the monkey and human substantia nigra: an intracellular renin-angiotensin system in the nigra. *Brain Struct Funct*. 2013;218:373–388.

42. Wu CY, Zha H, Xia QQ, et al. Expression of angiotensin II and its receptors in activated microglia in experimentally induced cerebral ischemia in the adult rats. *Mol Cell Biochem*. 2013;382:47–58.

43. Kettenmann H, Hanisch UK, Noda M, Verkhratsky A. Physiology of microglia. *Physiol Rev*. 2011;91:461–553.

44. Miyoshi M, Miyano K, Moriyama N, Taniguchi M, Watanabe T. Angiotensin type 1 receptor antagonist inhibits lipopolysaccharide-induced stimulation of rat microglial cells by suppressing nuclear factor kappaB and activator protein-1 activation. *Eur J Neurosci*. 2008;27:343–351.

45. Hatzopoulos KM, Vessey KA, Wilkinson-Berka JL, Fletcher EL. The vasoneuronal effects of AT1 receptor blockade in a rat model of retinopathy of prematurity. *Invest Ophthalmol Vis Sci*. 2014;55:3957–3970.

46. Al-Merani SA, Brooks DP, Chapman BJ, Munday KA. The half-lives of angiotensin II, angiotensin II-amide, angiotensin III, Sar1-Ala8-angiotensin II and renin in the circulatory system of the rat. *J Physiol*. 1978;278:471–490.

47. van Kats JP, de Lannoy LM, Jan Danser AH, van Meegen JR, Verdouw PD, Schalekamp MA. Angiotensin II type 1 (AT1) receptor-mediated accumulation of angiotensin II in tissues and its intracellular half-life in vivo. *Hypertension*. 1997;30:42–49.

48. Bhat SA, Goel R, Shukla R, Hanif K. Angiotensin receptor blockade modulates NFkappaB and STAT3 signaling and inhibits glial activation and neuroinflammation better than angiotensin-converting enzyme inhibition. *Mol Neurobiol*. 2016;53:6950–6967.

49. Lanz TV, Ding Z, Ho PP, et al. Angiotensin II sustains brain inflammation in mice via TGF-beta. *J Clin Invest*. 2010;120:2782–2794.

50. Le W, Rowe D, Xie W, Ortiz I, He Y, Appel SH. Microglial activation and dopaminergic cell injury: an in vitro model relevant to Parkinson's disease. *J Neurosci*. 2001;21:8447–8455.

51. Sano M, Fukuda K, Kodama H, et al. Interleukin-6 family of cytokines mediate angiotensin II-induced cardiac hypertrophy in rodent cardiomyocytes. *J Biol Chem*. 2000;275:29717–29723.

52. Rojas M, Zhang W, Lee DL, et al. Role of IL-6 in angiotensin II-induced retinal vascular inflammation. *Invest Ophthalmol Vis Sci*. 2010;51:1709–1718.

53. Fouda AY, Artham S, El-Remessy AB, Fagan SC. Renin-angiotensin system as a potential therapeutic target in stroke and retinopathy: experimental and clinical evidence. *Clin Sci (Lond)*. 2016;130:221–238.

54. Rymo SF, Gerhardt H, Wolfhagen Sand F, Lang R, Uv A, Betsholtz C. A two-way communication between microglial cells and angiogenic sprouts regulates angiogenesis in aortic ring cultures. *PLoS One*. 2011;6:e15846.

55. Fantin A, Vieira JM, Gestri G, et al. Tissue macrophages act as cellular chaperones for vascular anastomosis downstream of VEGF-mediated endothelial tip cell induction. *Blood*. 2010;116:829–840.

56. Kremlev SG, Roberts RL, Palmer C. Differential expression of chemokines and chemokine receptors during microglial activation and inhibition. *J Neuroimmunol*. 2004;149:1–9.

57. Prinz M, Priller J. Tickets to the brain: role of CCR2 and CX3CR1 in myeloid cell entry in the CNS. *J Neuroimmunol*. 2010;224:80–84.

58. O'Koren EG, Mathew R, Saban DR. Fate mapping reveals that microglia and recruited monocyte-derived macrophages are definitively distinguishable by phenotype in the retina. *Sci Rep*. 2016;6:20636.

59. Vessey KA, Greferath U, Aplin FP, et al. Adenosine triphosphate-induced photoreceptor death and retinal remodeling in rats. *J Comp Neurol*. 2014;522:2928–2950.

60. Nakazawa T, Shimura M, Endo S, Takahashi H, Mori N, Tamai M. N-Methyl-D-Aspartic acid suppresses Akt activity through protein phosphatase in retinal ganglion cells. *Mol Vis*. 2005;11:1173–1182.

61. Marin-Teva JL, Cuadros MA, Calvente R, Almendros A, Navascues J. Naturally occurring cell death and migration of microglial precursors in the quail retina during normal development. *J Comp Neurol*. 1999;412:255–275.

62. Wang X, Zhao L, Zhang J, et al. Requirement for microglia for the maintenance of synaptic function and integrity in the mature retina. *J Neurosci*. 2016;36:2827–2842.